Korean J. Chem. Eng., **23**(1), 124-130 (2006)

Modeling of protein adsorption to DEAE sepharose FF: Comparison of data with model simulation

Mohammad Reza Aboudzadeh†, Zhu Jiawen* and Wu Bin*

Nuclear Research Center for Agriculture & Medicine, AEOI, P.O. Box 31585-4395, Karaj, Iran
*Chemical Engineering Research Center, East China University of Science and Technology, Shanghai, 200237, P.R. China
(*Received 9 June 2005 • accepted 4 October 2005*)

Abstract−The equilibrium and kinetic characteristics of the adsorption of human serum albumin (HSA) and ovalbumin (OVA) to the DEAE Sepharose FF weak anion exchanger were experimentally determined. The rate for protein adsorption was simulated with two different models, the first being based on a single lumped kinetic parameter, while the second includes the individual mass transfer processes occurring prior to the adsorption intervention, i.e., diffusion across the liquid film surrounding individual particles and diffusion within the ion exchanger particle itself. The actual adsorption of OVA to DEAE Sepharose FF in fully mixed stirred vessels and in packed bed columns was consistent with both models. In the case of HSA, however, the adsorption profile in an agitated vessel was consistent only with the pore diffusion model and neither model could correctly predict the latter part of the breakthrough profile observed in packed bed experiments.

Key words: Ion Exchange Chromatography, Breakthrough, Stirred Vessel, Packed Bed, Langmuir, HSA, OVA

INTRODUCTION

The first theoretical models of chromatography are dated from the late 1930s and early 1940s. The pioneering works [Wicke and Kolloid, 1940; Wilson, 1940; De Vault, 1943; Martin and Synge, 1941; Martin and James, 1952; Craig, 1944] began approaches to developing and improving our understanding of chromatography. Linear *kinetic rate constant model* was first tread by Wilson, 1940, Weiss, 1943 and De Vault, 1943 extended this model to nonlinear chromatography. Any hydrodynamic dispersion or mass transfer effects are neglected at this model. If we consider zone spreading effects, a more rigorous model, called a *film and pore diffusion model* is derived.

Bohart and Adams derived the equations of the film and pore diffusion model as early as 1920, but it does not seem that they attempted any calculations based on this model [Bohart and Adams, 1920]. Wicke and Kolloid derived the same model equation in 1939 and discussed its application to gas chromatography on activated charcoal [Wicke and Kolloid, 1939, 1940]. The model has no analytical solutions. It was only around 1987 that the calculation of the band profiles of single compounds and binary mixtures began to become accessible [Guiochon et al., 1988].

In the production of biopharmaceutical proteins, chromatography is a common method of choice as one of the last steps in purification. Ion exchange adsorbents have found widespread use in the purification of proteins since the introduction of the first ion exchanger specifically designed for proteins in 1951 [Hirs et al., 1951]. The extensive use of ion exchangers is due to their versatility, low cost, and the acceptance of regulatory authorities for use in the production of pharmaceutical proteins. This is in contrast to affinity adsorbents, which are expensive and only limited to use in purification of one or a group of proteins. For example, in the purification of recombinant human serum albumin (rHSA), chromatography is used for removal of HSA from impurity [Ohinura, 1996]. HSA is the most abundant protein in human blood, serving as a transport protein and as a driving force for osmotic transport. Li and Pinto have presented a thermodynamically consistent adsorption equilibrium model based on the stoichiometric displacement principle that has been developed for nonlinear protein ion exchange [Li and Pinto, 1994].

In this work, the effect of properties of ion exchangers on adsorption performance was investigated and simple models of the purification process were constructed to assist process design. Experimental data was obtained from the adsorption of HSA and OVA with DEAE Sepharose FF weak anion exchanger, and the experimental results were compared to simulation results with two different models for description of the adsorption process.

The adsorption isotherm, i.e., the equilibrium adsorption capacity of DEAE Sepharose FF for each of the proteins, was determined. Since the adsorption of proteins by an ion exchanger is not an instantaneous event, the rate of adsorption of proteins in a mixing vessel was studied to examine mass transfer effects. Finally, the adsorption of protein in a column packed with DEAE Sepharose FF was determined through breakthrough profiles.

THEORY

1. Equilibrium Model

In analysis of protein adsorption to ion exchangers, the adsorbent is frequently assumed to consist of functional groups of electric charges which are balanced by associated counter-ions, while the protein molecule is assumed to exist in an ionized state in solution. Upon adsorption onto an ion exchanger, a protein molecule displaces the counter-ions previously associated with the ion exchanger matrix. For an ion exchanger equilibrated with monovalent counter-

†To whom correspondence should be addressed.
E-mail: aboudzadeh@yahoo.com

ions, this process can be represented by the following equation:

$$A \cdot nI + P^{n} \leftrightarrow A \cdot P + nI \tag{1}$$

Where A represents the adsorption site on the ion exchanger, I represents the counter-ions, P the protein molecule and n the number of charges involved in the interaction with each adsorbed protein molecule. If the change in bulk fluid concentration of the counter-ion I is small as a result of protein adsorption onto the ion exchanger, as is the case when buffered solutions containing I are used, then adsorption equilibrium as shown in Eq. (1) may be simplified to:

$$A + P \underset{k_{-1}}{\overset{k_1}{\rightleftharpoons}} A \cdot P \tag{2}$$

And hence, the rate for the change of the adsorbed protein concentration is given by:

$$\frac{dq}{dt} = k_1 c(q_m - q) - k_{-1} q \tag{3}$$

Where c is the soluble protein concentration, k_1 and k_{-1} are the adsorption and desorption rate constants, q is the adsorbed protein concentration, q_m is the maximum adsorption capacity of protein by the ion exchanger.

While equilibrium is achieved, dq/dt=0, and hence the following can be derived from Eq. (3):

$$q^{*} = \frac{k_1 c^{*} q_m}{k_1 c^{*} + k_{-1}} \tag{4}$$

In which the superscript * denotes values when equilibrium has been established between the solid and mobile phase. Substitution of $K_d = k_{-1}/k_1$ into Eq. (4) gives:

$$q^{*} = \frac{c^{*} q_m}{c^{*} + K_d} \tag{5}$$

Where K_d is the dissociation constant for the complex of protein with ion exchanger, i.e., A·P as shown in Eq. (1) and (2). Eq. (5) is the form of the Langmuir adsorption isotherm which is used frequently to describe the adsorption of protein to various adsorbents, including ion exchangers [Chen et al., 2003; Kaczmarski et al., 2001; Mao and Hearn, 1996]. Rearrangement of Eq. (5) gives the linear form of

$$\frac{c^{*}}{q^{*}} = \frac{K_d}{q_m} + \frac{c^{*}}{q_m} \tag{6}$$

From which, the dissociation constant, K_d and the maximum protein capacity of the ion exchanger, q_m, can be calculated by regression analysis of isotherm experimental data.

2. Modeling of Protein Adsorption

2-1. Kinetic Rate Constant Model

This model takes an empirical approach to the adsorption process and assumes that all of the rate limiting processes can be represented by kinetic rate constants. In this approach, the change of protein concentration in a batch operation of adsorption in a fully mixed stirred vessel can be obtained by substitution of c from mass balance equation (Eq. (7)) in Eq. (3):

$$cV = c_0 V - v q_m \tag{7}$$

and than analytical solution of Eq. (3), namely:

$$c = c_0 - \frac{v}{V}\left[\frac{(\xi - \varphi)\,1 - \exp\left\{-\frac{2\varphi v}{V} k_1 t\right\}}{1 - \left(\frac{\xi - \varphi}{\xi + \varphi}\right)\exp\left\{-\frac{2\varphi v}{V} k_1 t\right\}}\right] \tag{8}$$

Where

$$\varphi^2 = \xi^2 - \left(\frac{c_0 \cdot V}{v}\right) q_m \tag{9}$$

$$\xi = \frac{1}{2}\left(q_m + \frac{(c_0 + K_d)\cdot V}{v}\right) \tag{10}$$

c_0 is the initial concentration of protein in liquid phase, v is the volume of adsorbent, and V is the volume of liquid phase.

2-2. Film and Pore Diffusion Model

A more rigorous approach to modeling the adsorption process is to consider the different steps that occur during protein adsorption. These are commonly defined as transportation through the liquid film surrounding the adsorbent particles, diffusion within the pores of the adsorbent, and finally the adsorption reaction itself. The construction of the model is based on the following assumptions:

(1) The adsorbent is made of porous material into which the solute can only enter by diffusion. Effective pore diffusivity, D, is assumed to be independent of concentration and is based on the porosity of the adsorbent particle for small molecules, rather than the actual extent to which molecules of a particular protein penetrate the particle.

(2) Mass transfer from the bulk mobile phase to the surface of the adsorbent is governed by a film model characterized by a mass transfer coefficient, k_f.

(3) Surface reaction between the adsorbate and an adsorption site is described by a reversible second order reaction. Adsorption is isothermal, and its equilibrium behavior can be represented by the Langmuir equation. Surface diffusion in which adsorbate moves directly between adsorption sites without interim desorption into the liquid phase is assumed to occur at a negligible rate and hence a corresponding term is not required for description of this process.

(4) The adsorbent particles are spherical, with uniform size and density, and the functional groups of the ion exchanger are distributed evenly throughout the interior of the particle.

The mass balance for diffusion of protein in the liquid phase within the ion exchanger particle is shown as:

$$\frac{\partial c_i}{\partial t} + \left(\frac{1 - \varepsilon_p}{\varepsilon_p}\right)\frac{\partial q_i}{\partial t} = D\frac{1}{r^2}\frac{\partial}{\partial r}\left(r^2 \frac{\partial c_i}{\partial r}\right) \tag{11}$$

Where c_i is the point concentration of protein, ε_p is the particle porosity, q_i the point adsorbed quantity of protein and r the radial coordinate within the ion exchange particle. In this study, particle porosity was determined from knowledge of the solids content of the adsorbent. DEAE Sepharose FF is formulated from 6% agarose and hence the particle porosity was taken as 0.94 [Pharmacia LKB biotechnology].

The rate of mass transfer through the external film links the bulk liquid concentration, c, to the concentration in the liquid phase at the surface of the particle. The expression is shown as:

$$D\frac{\partial c_i}{\partial r}\bigg|_{r=R} = k_f(c-c_i)|_{r=R} \tag{12}$$

At the center of the particle,

$$r=0 \qquad \frac{\partial c_i}{\partial r}=0 \tag{13}$$

If a second order surface reaction rate is assumed, then the rate of change of adsorbed quantity of protein is given by Eq. (3) as above. At equilibrium this gives a form of the Langmuir equation with maximum capacity q_m and dissociation constant $K_d=k_{-1}/k_1$, Eq. (5).

For adsorption and desorption in a stirred tank, the rate of change of the bulk concentration of protein, c, is given by:

$$V\frac{dc}{dt} = -\frac{6k_fv}{d_p}(c-c_i)|_{r=R} \tag{14}$$

The correlation used to estimate the liquid film mass transfer coefficient, k_f, of protein to the adsorbent particles in stirred tank experiments is given by [Geankoplis, 1983]:

$$k_f = \frac{2D_{AB}}{d_p} + 0.31\left(\frac{\mu}{\rho D_{AB}}\right)^{-2/3}\left(\frac{\Delta\rho\mu g}{\rho^2}\right)^{1/3} \tag{15}$$

Where ρ is the particle density (1.06 g/cm^3), d_p is mean particle diameter (90 μm), $\Delta\rho$ is the density difference between the adsorbent particle and the liquid. The molecular diffusivity of OVA and HSA in free aqueous solution, D_{AB}, was estimated by using the following semi-empirical equation [Guichon, 1994]:

$$D_{AB} = 9.4\times10^{-15}\frac{T}{\mu(M_A)^{1/3}} \tag{16}$$

Where M_A is the relative molecular weight of substance A. Taking 44,000 and 67,000 as the relative molecular weight of OVA and HSA, respectively, the values of their molecular diffusion coefficients in phosphate buffer, D_{AB}, were found to be 7.9×10^{-11} m^2/s and 6.9×10^{-11} m^2/s at 293 °K, respectively.

For adsorption in a packed bed column, the individual band profile is obtained as the solution of the mass balance equation in a column. A mass balance is wrapped around a differential slice of the column. The model results from differential mass balances of the liquid (Eq. (17)) and the solid phase (Eq. (18)) [Huckman et al., 2001]:

$$\frac{\partial c}{\partial t} = D_x\frac{\partial^2 c}{\partial x^2} - u_o\frac{\partial c}{\partial x} - \frac{6k_f(1-\varepsilon_b)}{d_p\varepsilon_b}(c-c_i) \tag{17}$$

$$\frac{\partial q}{\partial t} = \frac{6k_f}{d_p}(c-c_i) \tag{18}$$

Where x is the axial coordinate in the bed, u_o the interstitial velocity of liquid in the bed ε_b and is the apparent bed voidage of the packed bed. Finally, the adsorption isotherm links liquid and solid equilibrium concentration (Eq. (5)). Using data from molecular-exclusion experiments, the porosity of packed beds of DEAE Sepharose FF was calculated to be 0.35.

The boundary conditions are derived from the assumption that mass transfer outside the column is caused by convection only. This leads to the Danckwerts boundary conditions [Danckwerts, 1953].

To study the importance of non ideal effect of axial dispersion in simulation of adsorption in a packed bed column, the axial diffusion term in Eq. (17) is once negligible and then considered.

To estimate film mass transfer coefficient (k_f) in a packed bed column, the following correlation proposed [Foo and Rice, 1975] was used:

$$Sh = 2+1.45Re^{1/2}Sc^{1/3} \tag{19}$$

Where $Sh=(k_fd_p)/D_{AB}$, $Re=(\rho u_0 d_p)/\mu$ and $Sc=\mu/(\rho D_{AB})$ are the Sherwood, the Reynolds and the Schmidt numbers, respectively.

The value of axial dispersions were calculated [Chung and Wen, 1968]

$$Pe = \frac{L}{2\varepsilon_b R}(0.2+0.0117*Re^{0.48}) \tag{20}$$

Where $Pe=(vd_p)/D_x$ is the Peclet number.

EXPERIMENTAL

1. Materials

HSA and OVA were obtained from the Shanghai Research Institute of Biochemistry and Bio Life Science & Technology Co., LTD. catalogue number G0070, respectively. HSA has a relative molecular weight of 67,000 Daltons and an isoelectric point (pI) of 4.9, while OVA has a relative molecular weight of 44,000 Daltons and pI of 4.7.

2. Adsorption Isotherms

Isotherms for the adsorption of each protein to DEAE Sepharose FF were determined in batch experiments. A known amount of DEAE which had been previously equilibrated with phosphate buffer (pH 6) was added to each of a series of flasks containing known volumes of buffered protein solution at different concentrations. The flasks were immersed in a thermostat at 293 °K to allow equilibrium to be established. After equilibrium was achieved, the agitation was stopped and the supernatant was sampled to determine the equilibrium concentration of protein with a UV spectrophotometer. The amount of protein adsorbed to the DEAE Sepharose FF was then calculated by using mass balance equations.

3. Kinetics of Batch Adsorption

The rate of adsorption of protein in a suspension of DEAE Sepharose FF was determined by continuously monitoring the soluble phase protein concentration in a batch system. The filtered liquid phase was continuously sampled from a fully mixed experimental vessel, passed through a UV spectrophotometer, and then returned to the experimental vessel. The experimental vessel was incubated in a shaking water bath at 293 °K. A typical experiment consisted of 50 ml of buffer containing protein at a concentration of 2 mg/ml. In order to achieve as rapid a response time as possible, the volume of the fluid sample was kept small (approximately 1 ml) and the solution was pumped at a flow rate of 7 ml/min. Experiments were started by the addition of 1 g of dry DEAE Sepharose FF into the protein solution. Output signal from the UV spectrophotometer was recorded by a chart recorder, and the protein concentration in the liquid phase at given time was determined from the chart recorder trace and reference to calibration data.

4. Frontal Analysis

Breakthrough curves were determined in order to evaluate packed bed performance. All of the column experiments were performed with 2 g of dry DEAE in buffer solution packed in a chromatogra-

phy column with an internal diameter of 1.5 cm and bed height about 1.3 cm, mounted vertically with a volumetric flow rate of 3 ml/min. A solution of 2 mg/ml protein (c_0) was fed into the column and optical density at 280 nm of the outlet stream was recorded. For the determination of breakthrough curves, the beds were loaded until the protein concentration in the outlet stream equaled, or was approaching, that of the inlet stream, c_0. At the end, protein was eluted from DEAE Sepharose FF with 1 M sodium chloride in 0.01 M phosphate buffer. Concentration of protein (c) in the outlet stream was plotted against time.

RESULTS AND DISCUSSION

1. Adsorption Isotherms

The isotherms for the adsorption of HSA and OVA to DEAE Sepharose FF in 0.01 M phosphate buffer, pH 6, are shown in Fig. 1. Data for both proteins are well described by a Langmuir isotherm; the parameters and are estimated by using Eq. (6) and obtained experimental results. They are shown in Table 1.

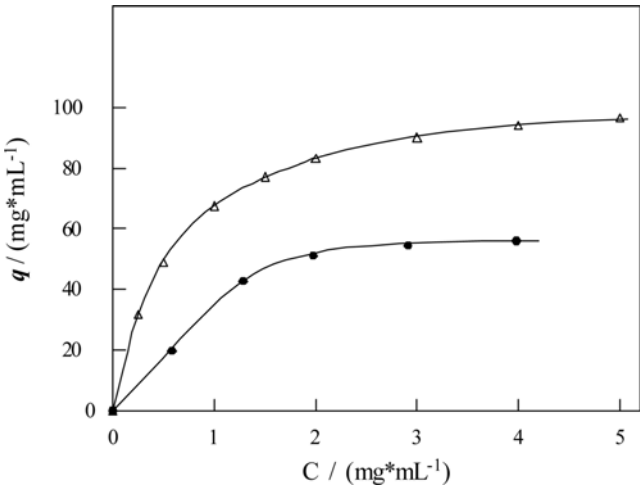

Fig. 1. Adsorption isotherm for ovalbumin (OVA) and human serum albumin (HSA) adsorbent: DEAE Sepharose FF. Liquid phase: 0.01 M Phosphate buffer, pH=6 at 293 K.
● — OVA; △ — HSA

Table 1. Values of constants for adsorption equilibrium of Human serum albumin (HSA) and ovalbumin (OVA) to DEAE Sepharose FF

	HSA	OVA
K_d (mg/ml)	0.604	0.423
K_d (mol)	9×10^{-6}	9.5×10^{-6}
q_m (mg/gr gel)	108.2	62.2
q_m (mol/*l*)	1.61×10^{-3}	1.41×10^{-3}
k_1 (ml/(mg.s))	4.9×10^{-4}	7.1×10^{-4}
k_1 (*l*/(mol.s))	32.83	31.24
k_f (m/s)[a]	5.6×10^{-6}	6.2×10^{-6}
k_f (m/s)[b]	5.5×10^{-6}	6.1×10^{-6}
D (m^2/s)	7.9×10^{-12}	1.1×10^{-11}
D_x (cm^2/min)	1×10^{-4}	9×10^{-5}

[a]Values obtain from the Eq. (15)
[b]Values obtain from the Eq. (19)

The equations of the kinetic rate constant model were solved with computation programs. The orthogonal collocation method on finite elements was used to solve the governing differential equations of the film and pore diffusion model [Baker, 1983]. The simulation results were compared with the experimental data. The obtained results are discussed in the following sections.

2. Kinetics of Adsorption in a Stirred Tank

Rates of protein adsorption in a stirred vessel were simulated with the two models described above: the kinetic rate constant model and the film and pore diffusion model. In each model, there was a single unknown parameter describing the rate of protein adsorption and the value of the parameter could be determined by correlation of the experimental data. With the kinetic rate constant model, a

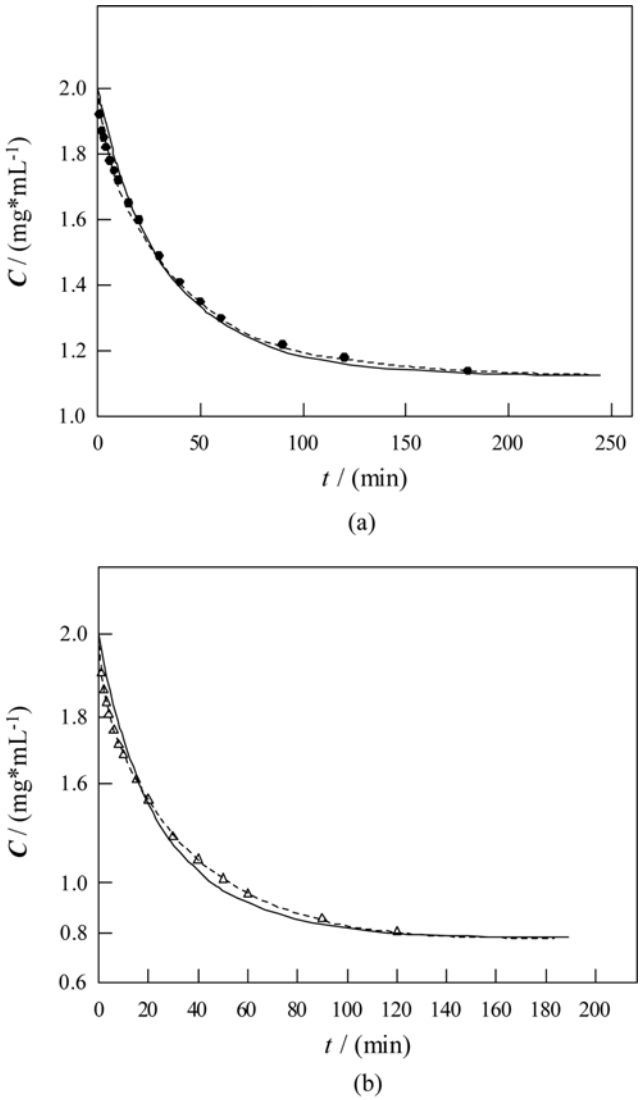

Fig. 2. Batch adsorption profiles for the adsorption of Ovalbumin and human serum albumin in suspension in agitated vessels.
(a) ● — OVA; (b) △ — HSA. adsorbent: DEAE Sepharose FF; —— adsorption profile predicted by the kinetic rate constant model; ------ adsorption profile predicted by the film and pore diffusion model

simulation of the protein adsorption rate was made by using Eq. (8). The only unknown parameter was the apparent rate constant, k_1 while values of the isotherm parameters q_m and K_d were determined by batch isotherm experiments and the other parameters were fixed in our experiments. k_{-1} is given simply by $K_d \cdot k_1$. The best fit value of k_1 was obtained from the correlation of experimental data of protein adsorption. Similarly, for the pore and diffusion model, simulation of the rate for protein adsorption was made by solving Eqs. (11)-(15) for the only unknown parameter D to find the value which gave the best fit of the experimental curve.

The agreement between the simulation result and the experimental adsorption curve is shown in Fig. 2. The best fit values for the rate constant, i.e., k_1 (for the kinetic rate constant model) and the effective diffusivity, D (for the film and pore diffusion model), are shown in Table 1. For the adsorption of OVA, it was possible to obtain a good fit with both models (Fig. 2a) within 5% accuracy; the simulated result of the film and pore diffusion model was found to match the experimental data more closely than that of the kinetic rate constant model.

The adsorption profile of HSA was also better described by the pore and film diffusion model (Fig. 2b, dashed line). With the kinetic rate constant model, the simulated absorption profile for HSA cannot approach the experiment point throughout the entire adsorption process (Fig. 2b, solid line). A possible reason for the relatively poor fit of the kinetic rate constant model to the HSA adsorption data is that diffusion of HSA within the adsorbent particles is hindered, and hence adsorption of HSA may occur initially in outer regions of particles. As the diffusion paths are short, adsorption appears to take place rapidly while the rate for later stages of adsorption, which must take place deeper inside the particles as the outer zones are filled with adsorbed molecules, is thus much slower than the initial rate. The OVA molecule, which is smaller than that of HSA, may be able to penetrate the particles more easily and adsorption could be proceeding at a more even rate throughout the whole adsorption period.

As expected, the values of the effective pore diffusion coefficient, D, were found to be lower than the calculated diffusion coefficient in free solution, D_{AB} for both proteins. The ratio of the molecular diffusivity in free solution, D_{AB}, to the effect diffusivity in the adsorbent particle, D, is 7.2 for OVA and 8.7 for HSA, which provides strong evidence that diffusion of HSA within the particle is more resisted than for the smaller OVA molecule. The relatively close agreement between theoretical and experimental profiles for both OVA and HSA suggests that the film and pore diffusion model is useful in the prediction of adsorption rate of proteins to ion exchangers in a fully mixed stirred vessel.

3. Frontal Analysis

Frontal analysis experiments were performed to see whether the two models of protein adsorption used in adsorption modeling in a stirred tank, could also describe the adsorption in a packed bed column. The experimental breakthrough data are shown in Fig. 3. The simulated curves by the two models using rate parameters determined in the batch adsorption experiments are also shown in the figure. However, the values of k_f used in the film and pore diffusion model were those appropriate for adsorption in a packed bed column and were estimated from the correlation given by Eq. (19).

For OVA, it was found that the pore and diffusion model gave a good fit to the experimental breakthrough data using the parameters derived from batch experiments (Fig. 3a, dashed line) within 10% accuracy. But, for HSA, neither of the two models gave a precise simulation of the breakthrough curve (Fig. 3b, solid line and dashed line).

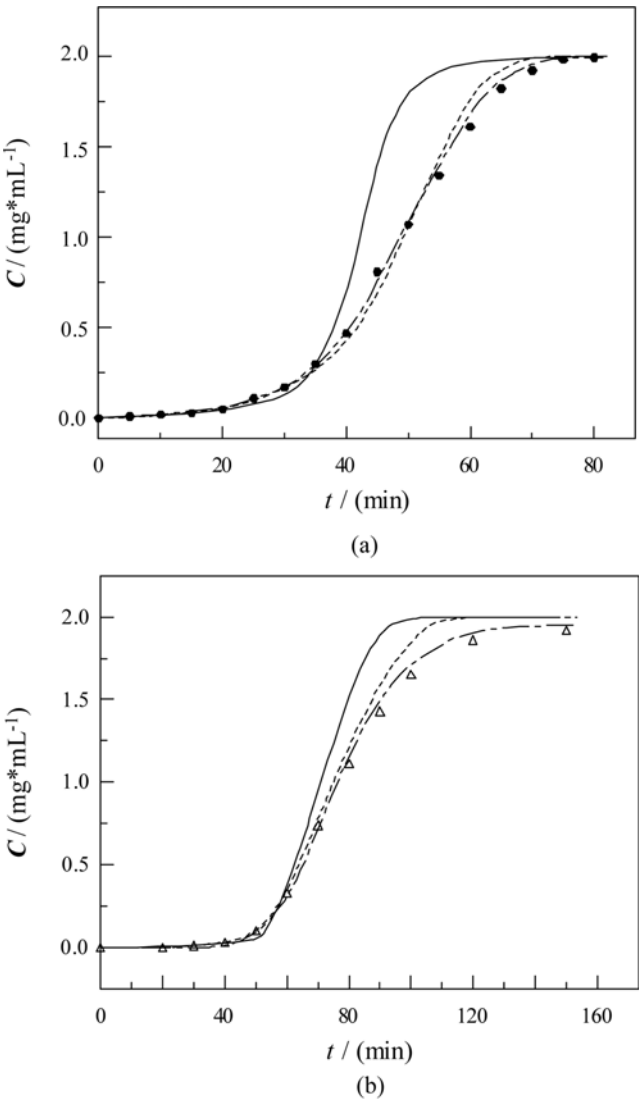

Fig. 3. Breakthrough profiles for the adsorption of Ovalbumin and human serum albumin in a packed bed column.
(a) ● — OVA; (b) △ — HSA. adsorbent: DEAE Sepharose FF. Column internal diameter: 1.5 cm, feed protein concentration: 2 mg/ml, flow rate: 2 ml/min. —— adsorption profile predicted by the kinetic rate constant model; ------ adsorption profile predicted by the film and pore diffusion model without axial dispersion; –––– adsorption profile predicted by the film and pore diffusion model with axial dispersion

The breakthrough curve for HSA was very asymmetric and the outlet concentration approached the inlet feed concentration very slowly. Indeed, it appeared that the equilibrium capacity of the bed for HSA was greater than that measured in batch experiment of adsorption isotherm. A value for maximum adsorption capacity could not be determined as the outlet concentration had not risen completely to the inlet value by the end of measurement. Both models fail

to predict the later part of breakthrough curve correctly, although the film and pore diffusion model did predict some degree of asymmetry to the shape of the curve and showed a good fit for the earlier part of the adsorption curve. The best fit with this model was obtained when the value of q_m used in the simulation was increased from the value found in batch adsorption experiments (108.2 mg/ml) to 128 mg/ml. The other rate parameters were also varied in an effort to obtain better fit to the experimental data: for the kinetic rate constant model, simulations were carried out with other values of k_1, and other values of D were used in the film and pore diffusion model. However, in both cases we were unable to obtain better a fit to the top end of the curve without resulting in a lack of fit with the earlier part of the experimental curve. As said before, since the OVA molecule has smaller size than has, therefore the larger HSA is restricted by ion exchanger particle more than OVA. So, attempts were also made to obtain better fits to the experimental data by using the non ideal effect of axial dispersion on the model's results. The good agreement between the simulation result and the experimental adsorption curve is observed in Fig. 3, dashed and dotted line, within 3% accuracy. It was found that this modified model can give a better fit to the experimental breakthrough than before. There is only a little deviation between them for HSA at the latter part of breakthrough profile.

As is discussed above, the ion exchanger might exhibit a greater adsorption capacity for HSA when loaded in a packed bed column than that predicted from batch adsorption isotherm experiments. This additional adsorption capacity appeared to be characterized by slow adsorption kinetics as evidenced by the slow rise in protein concentration during the later part of the breakthrough curve. The time-concentration profiles are different in a packed bed column and a stirred vessel experiments and this may partially explain the difference. It was reported that HSA can form dimer in solution [Foster et al., 1977], and it is possible that the high local concentrations of HSA that are present when the protein is adsorbed onto the ion exchanger, and the constant flow of fresh HSA solution into the packed bed column, may promote the formation of dimers. If this were the case, the apparent additional adsorption capacity may be the result of multi-layer binding of HSA molecules (partially in the form of dimers) in contrast to the single-layer adsorption in a stirred vessel experiment.

The results presented above illustrate the use of two different models to describe the adsorption of proteins to the weak anion exchanger DEAE Sepharose FF. The prediction from kinetic rate constant model and the film and pore diffusion model when neglecting the nonideal effect of axial dispersion for HSA adsorption is not as accurate as OVA adsorption, and it will be more accurate if the effect of nonideal axial dispersion is considered in the film and pore diffusion model. So it is strictly recommended to take a more rigorous approach for modeling the protein breakthrough profile by considering the axial dispersion effect in the film and pore model. Although it is recognized that the kinetic rate constant model is a gross simplification of the actual adsorption process, it may be a useful method only for the prediction of the adsorption of proteins to ion exchangers, as it is simple and suitable for estimation calculation where high precision is not imperative. Similar studies with an affinity adsorption system involving the adsorption of Urokinase to Sepharose 4B based affinity adsorbents showed that only the film and pore diffusion model described the experimental data accurately [Aboudzadeh et al., 2004].

CONCLUSION

In this study, the adsorption of HSA and OVA in a mixing vessel and a packed column was simulated and the simulation results were compared with the experimental results, which exhibit the validity of the adopted model. The following conclusion can be drawn from this research:

1. The adsorption rate of proteins to ion exchangers in a fully mixed stirred vessel can be predicted accurately with the film and pore diffusion model.
2. The kinetic rate constant model is a gross simplification of the actual adsorption process; it may be a useful method only for the prediction of the adsorption of proteins to ion exchangers.
3. There is more adsorption capacity for HSA in a fixed bed column than a stirred vessel that may be the result of multi-layer binding of HSA molecules (partially in the form of dimmers) in contrast to the single layer adsorption in a stirred vessel experiment.
4. This study shows that the OVA adsorption behavior in a fixed bed column is affected less than HSA by axial dispersion effect. So, this fact can be a strong reason for why the adsorption rate of HSA into adsorbent will be predicted accurately only when the effect of nonideality of axial dispersion is engaged into the film and pore diffusion model.
5. The behavior of protein adsorption in a fixed bed column is better predicted by more rigorous model such as film and pore diffusion model.

ACKNOWLEDGMENT

The authors are grateful to the National Natural Science Foundation of China for its funding of our research work through project No. 29976014. The Development Project of Shanghai Priority Academic Discipline also supported this work.

NOMENCLATURE

A : adsorption site on the ion exchanger
c : soluble protein concentration [mg/ml]
c_i : point concentration of protein [mg/ml]
c_0 : initial, or inlet liquid phase protein concentration [mg/ml]
d_p : mean particle diameter [m]
D : effective pore diffusivity [m^2/s]
D_{AB} : molecular diffusivity in free solution [m^2/s]
D_x : axial dispersion coefficient [m^2/s]
g : gravitational constant [m/s^2]
I : counter-ion
K_1 : adsorption rate constant [ml/(mg s)]
k_{-1} : desorption rate constant [s^{-1}]
k_f : liquid film Weiss mass transfer coefficient [m/s]
K_d : dissociation constant for the protein-ion-exchanger complex [mg/ml]
M_A : relative molecular weight of A
n : the number of charges involved in the interaction between

an adsorption site and a single protein molecule
P : protein molecule
q : concentration of protein adsorbed to the ion exchanger [mg/ml (adsorbent)]
q_i : point concentration of adsorbed protein [mg/ml (adsorbent)]
q_m : maximum protein capacity of the ion exchanger [mg/ml (adsorbent)]
r : radial coordinate of ion exchanger particle [m]
R : radius of ion exchanger particle [m]
Re : Reynolds number, $=u\rho d/\mu$
R_i : rate of interface mass transfer [m]
Sc : Schmidt number, $=\mu/(\rho D_{AB})$
Sh : Sherwood number, $=k_f d_p/D_{AB}$
t : time [s (min)]
T : absolute temperature [K]
u : superficial velocity of liquid flow through the column [m/s]
u_o : interstitial velocity of liquid in the bed [m/s]
V : volume of liquid external to the ion exchanger [ml]
x : axial coordinate of packed bed [m]
ε_p : porosity of ion exchanger particle
ε_b : porosity of packed bed
μ : liquid viscosity [kg/(ms)]
ρ : particle density [kg/m^3]

REFERENCES

Aboudzadeh, M. R., Jiawen, Z. and Wu, B., "Adsorption and step elution of urokinase using affinity chromatography-comparison of data with a rate model simulation," *Chinese J. Biomedical Eng.*, **13**(4), 166 (2004).

Baker, J., *Finite element computational fluid mechanics*, McGraw-hill, New York (1983).

Bohart, G. S. and Adams, E. Q., "Some aspects of the behavior of charcoal with respect to chlorine," *J. Am. Chem. Soc.*, **42**, 523 (1920).

Chen, W. D., Dong, X. Y., Bai, S. and Sun, Y., "Dependence of pore diffusivity of protein on adsorption density in anion-exchange adsorbent," *Biochem. Eng. J.*, **14**, 45 (2003).

Chung, S. F. and Wen, C. Y., "Longitudinal dispersion of liquid flowing through fixed and fluidized beds," *AIChE J.*, **14**, 857 (1968).

Craig, L. C., *J. Biol. Chem.*, 155,519, 1944, citied in Guichon, G. and Lin, B., *Modeling for preparative chromatography*, Academic press (2003).

Danckwerts, P. V., "Continuous flow systems: distribution of residence times," *Chem. Eng. Sci.*, **2**, 1 (1953).

De Vault, D., "The theory of chromatography," *J. Amer. Chem. Soc.*, **65**(4), 532 (1943).

Foo, S. C. and Rice, R. G., "On the prediction of ultimate separation in parametric pumps," *AIChE J.*, **21**, 1149 (1975).

Foster, J. F., Rosenoer, V. M., Oratz, M. and Rothschild, M. A., *Albumin structure, function and uses*, Pergamon Press, 53 (1977).

Geankoplis, C. J., *Transport processes and unit operations*, Allyn and Bacon, MA, 2nd Ed. (1983).

Guiochon, G., Golshan-Shirazi, S. and Jaulmes, A.,"Computer simulation of the propagation of a large-concentration band in liquid chromatography," *Anal. Chem.*, **60**, 1856 (1988).

Guichon, G., Shirazi, S. G. and Katti, A. M., *Fundamentals of preparative and nonlinear chromatography*, Academic Press, Boston, MA (1994).

Hirs, C. H. W., Moore, S. and Stien, W. H., "A chromatographic investigation of pancreatic ribonuclease," *J. Amer. Chem. Soc.*, **73**, 1893 (1951).

Huckman, M. E., Latheef, I. M. and Anthony, R. G., "Designing a commercial ion exchange carousel to treat DOE waste using CST granules," *AIChE J.*, **47**(6), 1425 (2001).

Kaczmarski, K., Antos, D., Sajonz, H., Sajonz, P. and Guiochon, G., "Comparative modeling of breakthrough curves of bovine serum albumin in anion exchange chromatography," *J. Chromatog.*, **925**, 1 (2001).

Li, Y. L. and Pinto, N. G., "Influence of lateral interactions on preparative protein chromatography I. Isothermal behavior," *J. Chromatog. A.*, **658**(2), 445 (1994).

Martin, A. J. P. and Synge, R. L. M., *Biochem. J.*, **35**, 1358 (1941), citied in Guichon, G., "Review: Preparative chromatography," *J. Chromatog.*, **969**, 129 (2002).

Martin, A. J. P. and James, A. T., "Gas-liquid partition chromatography: the separation and micro-estimation of ammonia and the methylamines," *Biochem. J.*, **50**, 679 (1952).

Mao, Q. M. and Hearn, M. T. W., "Optimization of affinity and ion-exchange chromatographic processes for the purification of proteins," *Biotech. Bioengin.*, **52**, 204 (1996).

Ohinura, T., *Recombinant human serum albumin process for producing the same and pharmaceutical preparation containing the same*, US Patent 5521287 (1996).

Pharmacia LKB biotechnology, Ion exchange chromatography, principle and method (1998).

Wicke, E. and Kolloid Z., 86(1939)295, citied in Guichon, G. and Lin, B., *Modeling for preparative chromatography*, Academic press (2003).

Weiss, J., *J. Chem. Soc.*, pp. 297, 1943, citied in Guichon, G. and Lin, B., *Modeling for preparative chromatography*, Academic press (2003).

Wicke, E. and Kolloid Z., 90(1940)156, citied in Guichon, G. and Lin, B., *Modeling for preparative chromatography*, Academic press (2003).

Wilson, J. N., "A theory of chromatography," *J. Amer. Chem. Soc.*, **62**(6), 1583 (1940).